Journal of Molecular Structure 1234 (2021) 130201

Contents lists available at ScienceDirect

Journal of Molecular Structure

journal homepage: www.elsevier.com/locate/molstr

Bis-sulfonyl-chalcone-BODIPY molecular probes for *in vivo* and *in vitro* imaging

Zhixiang Lv[a], Yuling Wang[d], Jinliang Zhang[b], Zhou Wang[c], Guofan Jin[d,*]

[a] The People's Hospital of Danyang, Affiliated Danyang Hospital of Nantong University, Zhenjiang, 212300, P.R. China
[b] Zhucheng Maternal and Child Health Hospital, Zhucheng 262200, P.R. China
[c] College of Vanadium and Titanium, Panzhihua University, 617000, P.R. China
[d] School of Pharmacy, Jiangsu University, Zhenjiang 212013, P.R. China

ARTICLE INFO

Article history:
Received 7 January 2021
Revised 19 February 2021
Accepted 22 February 2021
Available online 28 February 2021

Keywords:
Bis-sulfonyl chalcone-BODIPY
Fluorescence sensor
Target cell imaging
Cell permeability
Molecular docking study

ABSTRACT

BODIPY derivatives have attracted much attention in cell imaging, so its excellent cell permeability has become the focus of extensive research. In this paper, different bis-sulfonyl chalcone-BODIPYs cell targeting probes were designed, synthesized and characterized. The cell viability experiment, cell imaging, flow cytometry, apoptosis, and *in vivo* experiments in mice were conducted to analyze them. The results showed that bis-methanesulfonyl chalcone-BODIPY had better activity evaluation on HeLa cells, and the data of IC_{50} decreased from 79.71 ± 3.84 to 56.10 ± 8.51. The three compounds have amazing cell imaging, especially compounds **5** and **6** are combined with the nucleus completely, showing strong cell permeability. In addition, *in vivo* imaging of mice experiments showed strong fluorescence and potential tumor targeting. In the molecular docking simulation, compounds **5** and **6** have high affinity scores with CDK2 of tumor cells: -8.4 and -8.6 kcal•mol^{-1}, and there are hydrogen bond, π - π, T - π, hydrophobic bond, ion-π and other interactions between them, which can well bind the compounds to the targets. These results indicate that bis-sulfonyl chalcone-BODIPYs have promising targeting capability and biocompatibility.

1. Introduction

In recent years, the field of targeted probes has become more and more abundant, but most probes have strong cytotoxicity and low cell permeability. To improve the probe, researchers often introduce small molecules or groups. Chalcone is a kind of small molecule substance widely existing in natural products. The framework of α, β-unsaturated ketone skeleton with two benzene rings has attracted the attention of chemists and pharmacists due to its unique structure and wide range of physiological activities [1–3]. The α, β-unsaturated carbonyl group in chalcone makes it have biological activity, therefore its derivatives show important anti-tumor, anti-cancer, antibacterial, anti-inflammatory, antimalaria and antiviral properties. Its derivatives can inhibit the formation of thrombin showed the potential activity against plasmodium falciparum [4]. It can also be used as the precursor of flavonoids and isoflavones, or designed as the synthesizers of novel heterocyclic compounds and a series of drug analogues [5].

Sulfonyl group is a good leaving group [6], and its derivatives have extensive anti-inflammatory and anti-tumor activities, so it is widely used in drug modification. Noscapine was modified with benzenesulfonyl to improve its biocompatibility with tubulin protein and its anti-proliferative activity against different tumor cells [7]. BODIPY is modified with sulfonyl to enhance the water-soluble and biological compatibility of the dye, which can be better used for membrane potential imaging [8]. In addition, sulfonyl-containing drugs such as antibacterial, anti-inflammatory, and anti-tumor are widely used in clinical [9–11], hence, it can be seen that the reasonable introduction of small molecules or groups in the compound design will have an incredible effect.

Among the targeted probes, BODIPY is a kind of typical high fluorescence dye, which involves a wide range of research fields, such as material research, medical research, medical diagnosis and treatment, environmental detection and so on. Compared with other fluorescent materials, it has high fluorescence quantum yield, good light stability, strong absorption and emission [12–14], appropriate stokes shift, and even its maximum absorption peak can reach the near-infrared region after certain modification [15–17]. It is one of the most promising dyes to improve photodynamic therapy (PDT) [18,19], making use of its good stability characteristics to

* Corresponding author:
E-mail address: organicboron@ujs.edu.cn (G. Jin).

https://doi.org/10.1016/j.molstruc.2021.130201
0022-2860/

produce hypoxia sensors or hydroxylamine [20], lactic acid sensors [21, 22]. Up to now, BODIPY derivatives have been proved to be promising bioanalytical reagents for *in-vivo* fluorescence imaging and diagnosis, and have been used for DNA and protein labeling widely [23–26]. However, The BODIPY probe itself is toxic, and it has been a long cherished wish of researchers in this field to seek BODIPY with lower toxicity and higher cell permeability.

Herein, we designed different bis-sulfonyl chalcone-BODIPY fluorescent probes to reduce the toxicity and improve the biocompatibility of target. The cytotoxicity of the three compounds to HCT-116 and HeLa cancer cells was determined by MTT assay. In order to understand its biological imaging more comprehensively, we conducted molecular docking, cell experiment *in vitro*, flow cytometry, apoptosis experiment and *in vivo* experiment in mice. In addition, the three compounds synthesized by us have the potential properties of chalcone drugs, which will be a new breakthrough in the field of BODIPY research.

2. Experimental section

2.1. Reagents and instrumentation

All solvents are commercially purchased and further purified. Dichloromethane and acetonitrile were distilled over calcium hydride. All the reaction products were separated and purified by column chromatography (200-300 mesh silica gel). The reaction process was detected by TLC and analyzed by UV lamp at 254 nm and 365 nm. NMR were measured by Bruker avance II instrument in deuterium chloroform (400 MHz for ^{1}H and 100 MHz for ^{13}C). Chemical shifts are reported in ppm, versus internal tetramethylsilane as a standard. The mass spectrum of **4** was obtained on a Thermo LXQ by liquid chromatgraphy-ion trap mass spectrometry, and the high resolution mass spectrometry analysis of **5** and **6** was performed by Micromon technical corporation, China. The infrared of the samples was recorded by Nicolet avato-370 FT-IR analyzer and tested by KBr tablet. UV-Vis absorption spectroscopy were recorded by UV-2550 spectrophotometer. The fluorescence emission spectra were recorded using a Shimadzu RF-5301PCS spectrofluorophotometer.

2.2. Synthesis

3-chloro-8-ethyl-5,5-difluoro-7,9-dimethyl-10-phenyl-5H-5λ^4,6λ^4-dipyrrolo[1,2-c:2′,1′-f][1,3,2]diazaborinine-2-carbaldehyde (2) [27]. N,N-Dimethylformamide (5 mL) and $POCl_3$ (5 mL) were mixed and stirred for 5 min under the condition of ice water bath and argon protection. The mixture was continuously stirred for 30 min at room temperature. After that, **BODIPY-Cl** [28] (1.5 g, 4.2 mmol) and 1,2-dichloroethane (30 mL) were added and stirred at 50°C for 3 h. After cooling to room temperature, saturated $NaHCO_3$ aqueous solution was added slowly under ice bath conditions. Dichloromethane and water were added for extraction after stirring for 1 h at 25°C. Anhydrous $MgSO_4$ was added into the organic phase and filtered, and then separated by column chromatography (ethyl acetate: hexane = 40: 1) after vacuum distillation to afford **2** (1.33 g, 82%).

8-ethyl-5,5-difluoro-7,9-dimethyl-10-phenyl-3-(propylamino)-5H-5λ^4,6λ^4-dipyrrolo[1,2-c:2′,1′-f][1,3,2]diazaborinine-2-carbaldehyde (3) [27]. Acetonitrile (20 mL) and 1 drop of propylamine were added to **2** (1.0 g, 2.6 mmol) and stirred for 4 h at room temperature. After decompression spin evaporation, ethyl acetate and aqueous solution were added for extraction, and anhydrous $MgSO_4$ was added into the organic phase and filtered. **3** (1.35 g, 89%) was purified by flash chromatography (hexane: ethyl acetate = 30:1).

(E)-3-(1-(difluoroboranyl)-5-((Z)-(4-ethyl-3,5-dimethyl-2H-pyrrol-2-ylidene)(phenyl)methyl)-2-(propylamino)-1H-pyrrol-3-yl)-1-(2,4-dihydroxyphenyl)prop-2-en-1-one (4). 20 mL acetonitrile was added into **3** (1.0 g, 2.43 mmol) and 1-(2,4-dihydroxyphenyl) ethan-1-one (1.11 g, 7.29 mmol), 0.5 mL piperidine was added dropwise under magnetic stirring, and the reaction was stopped after reflux at 80°C for 2 h. After the reaction was confirmed by TLC, the reaction solution was cooled to room temperature and product (0.3 g, 25%)was purified by column chromatography (petroleum ether: ethyl acetate = 8: 1). ^{1}H NMR (400 MHz, $CDCl_3$): δ (ppm) = 7.22 (t, J = 7.6 Hz, 2H), 7.08 (d, J = 6.8 Hz, 1H), 6.08 (d, J = 8.0 Hz, 1H), 6.11 (d, J = 8.0 Hz, 2H), 5.94 (s, 1H), 5.86 (s, 1H), 3.30 (s, 1H), 2.68 (d, J = 8.8 Hz, 6H), 2.47 (s, 2H), 2.34-2.29 (m, 2H), 1.57 (q, J = 7.2 Hz, 2H), 1.28 (d, J=5.2 Hz, 4H), 0.97 (t, J = 7.6 Hz, 3H), 0.86 (t, J = 7.6 Hz, 3H). ^{13}C NMR (100 MHz, $CDCl_3$): δ (ppm) = 205.7, 160.3, 158.8, 158.0, 143.3, 135.5, 135.2, 132.6, 131.3, 130.5, 129.7, 129.6, 128.2, 127.9, 125.1, 120.8, 110.2, 106.6, 45.6, 40.4, 34.1, 33.4, 29.7, 24.2, 17.2, 15.0, 11.8, 11.4, 10.8. FT-IR ν/cm^{-1}: 3443, 2923, 2360, 1600, 1437, 1373, 1334, 1221, 1125, 1043. ITMS (ESI$^+$) m/z: [M+H]$^+$ calcd for $C_{31}H_{32}BF_2N_3O_3$ 544.2583, found 544.3423.

(E)-4-(3-(8-ethyl-5,5-difluoro-7,9-dimethyl-10-phenyl-3-(propylamino)-5H-5λ^4,6λ^4-dipyrrolo[1,2-c:2′,1′-f][1,3,2]diazaborinin-2-yl)acryloyl)-1,3-phenylene dimethanesulfonate (5). 4 (0.1 g, 0.18 mmol) was dissolved in 8 mL dichloromethane solution. Triethylamine (0.15 mL, 1.08 mmol) and methylsulfonyl chloride (70 μL, 0.90 mmol) were added under magnetic stirring at room temperature, and the reaction was stopped after the white smoke dispersed. Orange red solid **5** (60 mg, 47%) was obtained using column separation and purification (petroleum ether: ethyl acetate = 3: 1). ^{1}H NMR (400MHz, $CDCl_3$): δ (ppm) = 7.33 (t, J = 6.0 Hz, 3H), 7.20 (d, J = 8.0 Hz, 2H), 7.15 (d, J = 8.8 Hz, 2H), 6.80 (d, J = 8.4 Hz, 2H), 6.11 (s, 1H), 5.79 (s, 1H), 3.21 (s, 5H), 2.76 (s, 5H), 2.46 (s, 3H), 2.33-2.28 (dd, J = 14.8 Hz, 7.2 Hz, 2H), 1.32 (s, 3H), 0.97 (t, J = 7.2 Hz, 3H), 0.89 (t, J = 7.2 Hz, 3H).^{13}C NMR (100 MHz, $CDCl_3$): δ (ppm) = 203.6, 161.0, 157.3, 147.8, 144.6, 143.5, 135.1, 134.6, 132.6, 132.1, 132.0, 130.3, 129.9, 129.8, 129.7, 128.2, 127.9, 122.5, 114.5, 111.8, 45.6, 38.5, 35.0, 32.5, 24.3, 17.1, 15.0, 11.9, 11.5, 10.8. FT-IR ν/cm^{-1}: 2928, 2363, 1593, 1460, 1373, 1215, 1182, 1122, 1023. TOF-MS (ES$^+$) m/z: [M+H]$^+$ calcd for $C_{33}H_{36}BF_2N_3O_7S_2$ 700.2134, found 700.2139.

(E)-4-(3-(8-ethyl-5,5-difluoro-7,9-dimethyl-10-phenyl-3-(propylamino)-5H-5λ^4,6λ^4-dipyrrolo[1,2-c:2′,1′-f][1,3,2]diazaborinin-2-yl)acryloyl)-1,3-phenylene dibenzenesulfonate (6). 4 (0.1 g, 0.18 mmol) was dissolved in 8 mL dichloromethane solution, and triethylamine (0.15 mL, 1.08 mmol) and benzenesulfonyl chloride (120 μL, 0.94 mmol) were dropped under magnetic stirring at room temperature. The reaction was stopped after the reaction was confirmed by TLC. Purplish red solid **6** (75 mg, 50%) was obtained by column chromatography (petroleum ether: ethyl acetate = 5: 1). ^{1}H NMR (400MHz, $CDCl_3$): δ (ppm) = 8.06 (d, J = 8.0 Hz, 3H), 7.78-7.69 (m, 4H), 7.66-7.59 (m, 6H), 7.45-7.41 (m, 5H), 5.93 (s, 1H), 5.67 (s, 1H), 2.53 (s, 2H), 2.37 (d, J = 6.4 Hz, 6H), 1.51-1.43 (m, 2H), 1.39-1.28 (m, 5H), 1.04 (t, J = 7.6 Hz, 3H), 0.77 (t, J = 7.6 Hz, 3H). ^{13}C NMR (100 MHz, $CDCl_3$): δ (ppm) = 196.9, 156.4, 145.7, 144.4, 142.8, 135.3, 135.2, 135.1, 134.1, 132.3, 132.0, 131.8, 131.3, 130.1, 129.7, 129.6, 129.4, 129.4, 128.7, 128.5, 128.3, 128.3, 127.0, 122.0, 121.1, 60.4, 53.5, 46.2, 36.0, 31.5, 30.2, 23.1, 17.3, 15.0, 12.0, 11.5, 10.9. FT-IR ν/cm^{-1}: 2923, 2360, 1710, 1592, 1458, 1383, 1216, 1188, 1083. TOF-MS (ES$^+$) m/z: [M+H]$^+$ calcd for $C_{43}H_{40}BF_2N_3O_7S_2$ 824.2447, found 824.2446.

2.3. Cytotoxicity determination

HCT-116, HeLa, and normal liver L-02 cells from American type culture collection were screened for cytotoxicity *in vitro*. HCT-116

and HeLa cells were routinely cultured in RPMI-1640 medium, while L-02 cells were routinely cultured in dulbecco's modified eagle medium (DMEM). 10% fetal bovine serum (FBS) was added to the medium, and the cells were incubated a cell incubator at 37°C with 5% carbon dioxide. These cells were monitored daily and maintained cell density at 80%.

The cytotoxicity of HCT-116, HeLa cells and normal lung L-02 cells were measured at logarithmic growth phase with different compounds. All cells were inoculated into 96-well plates at a rate of 106 cells per well. The samples were then treated with compounds and berberine at different concentrations and incubated at 37°C and 5% carbon dioxide for 24 h. Add 100 mL dimethyl sulfoxide to the supernatant of the sample and shake well for 10 min. The optical density of the sample was measured at 490 nm with a microplate photometer. Cell viability was expressed by the percentage change of absorbance relative to the control value.

2.4. Cell imaging

Cell inoculation: HeLa cells in the logarithmic growth phase were digested with trypsin and seeded into a 6-well plate containing round cap, which was cultured in an incubator at 5% CO_2 and 37°C for 24 h before adhering. Drug treatment: **4**, **5**, **6** samples were weighed and added into dimethyl sulfoxide (C = 0.25 mmol L^{-1}) and diluted to 2.5 μmol L^{-1} respectively. Dosing process: discard the original culture medium for each well cell and replace it with medium containing 2.5 μmol L^{-1} of a different drugs. Cell treatment: the medium was discarded and washed twice with phosphate buffer saline (PBS) after 24 h. The fixative was added with paraformaldehyde for 10 min, and the fixative was carefully sucked out. Wash it with PBS twice, and incubate with DAPI dye for 10 min under dark condition. The staining solution was discarded and washed with PBS twice again. After the tablets were sealed with anti-fluorescence quenching sealant, the samples and nuclear changes were observed under fluorescence microscope.

2.5. In vivo *imaging*

In vivo imaging experiments were performed on a single mouse component weighing 20 g and 7 weeks old. **5** (25 μmol L^{-1}, 25 μL in 1: 9 dimethyl sulfoxide/ saline, V/V) was injected on an empty stomach for 30 min. The fluorescence intensity of subcutaneous tumor tissues was then detected. In addition, the mouse experiment meets the requirements of animal ethics (the ethics committee approval No. syxk 2018-0053).

2.6. Flow cytometry analysis

HeLa cells cultured in 12-well petri dish were treated with **5**. Then the cell suspension was incubated with trypsin at 37°C for 12 h. It was placed in precooled 75% ethanol at 25°C below zero overnight. Ribozyme (10 μg mL^{-1}) and propidium iodide (15 nmol L^{-1}, PI); BD Biosciences (Anolun Biotechnology Co., Ltd, Beijing) was added to the cells for dark incubation at room temperature for 30min. The samples were then evaluated using flow cytometry (ATTUNE NXT, Life tech, Inc). ModFit LT 2.0 software (Verity Software House, Inc., Topsham, ME, USA) was used for data analysis.

2.7. Apoptosis

Compound 5 was used to treat HeLa cells cultured in a 12-well petri dish. Cell suspension was collected by trypsin at 37°C without ethylene diamine tetraacetic acid (EDTA). After washing with PBS, 250 mL binding buffer was added for resuspension. The Cell suspension was stained with 5 μL fluorescent protein PI and 5 μL Annexin V isothiocyanate solution (Yassen Biotechnology Co., LTD., Shanghai). Then they were incubated in dark at room temperature for 25 min and detected by flow cytometry (ATTUNE NXT, Lifetech, Inc). All test methods are in triplicate.

3. Results and discussion

3.1. Design and synthesis of target compounds

To synthesize the designed bis-sulfonyl chalcone-dipyrromethene boron difluoride, we took 3-chloro-5,7-dimethyl-6-ethyl-8-phenyl-BODIPY as the crude material (Scheme 1), catalyzed by $POCl_3$. Formyl group was introduced into the pyrrole ring containing chlorine to get **2**. The nucleophilic substitution reaction of **2** and propylamine, obtained **3** in 89% yield with acetonitrile as solvent. The introduction of propylamino group in this step is expected to better increase the drug activity of the compounds. Then, **4** was synthesized by condensation reaction of BODIPY with aldehydes group and 1-(2,4-dihydroxyphenyl)ethan-1-one with α-H, catalyzed by piperidine. Finally, bis-sulfonyl-chalcone-BODIPYs were synthesized by reacting with methanesulfonyl chloride and benzenesulfonyl chloride respectively under the catalysis of triethylamine in dichloromethane.

3.2. Spectroscopic properties

3443 cm^{-1} (ν, O-H) in compound **4** is the stretching vibration peak of phenolic hydroxyl group (Fig. 1 and Fig. S1-S3). The characteristic absorption peak of B-F in BODIPY is around 1268 cm^{-1}, 1119 cm^{-1} and 1043 cm^{-1} [29]. Around 1370 cm^{-1} (ν_{as}, SO_2), 1180 cm^{-1} (ν_s, SO_2) is the symmetric and anti-symmetric stretching vibration peak of R-SO_2-R [30]. This indicates the successful introduction of sulfonyl group to compounds **5** and **6**. In addition, the color differences of the compounds are shown in Fig. 1b. The interesting thing is that compound 5 has a flake like feel of gold foil, which reflects red and orange under light.

We discussed the full wavelength absorption and emission spectra of **4, 5, 6** in dichloromethane, as shown in the supporting information Figure S4. The ultraviolet absorption of the three compounds synthesized by us increases with the increase of compound concentration, while the maximum ultraviolet absorption wavelength is basically unchanged, all within the range of 540-548 nm. The concentration of the compound is proportional to its fluorescence. However, at the same excitation wavelength (λ_{ex} = 500 nm), there is no significant change in the peak shape or emission wavelength of the three compounds. This indicates that the introduction of sulfonyl group has no obvious effect on the fluorescence properties of the compounds.

Compound **4** has a maximum ultraviolet absorption at 545 nm and an emission maximum at 569 nm (Fig. 2a and Table 1). Compound **5** has a maximum linear absorption at 548 nm and maximum emission wavelength of 569 nm (the three compounds are all at λ_{ex} = 500 nm). The maximum linear absorption of compound **6** is 540 nm and the emission peak is at 566 nm. Stokes shift of the three compounds were all around 20 nm. Under sunlight, the three compounds were red in dichloromethane solution and showed a very strong orange-red fluorescence under ultraviolet light of 365 nm. In addition, the fluorescence quantum yields of all BODIPY derivatives were evaluated in dichloromethane solution in table 1, and the compound **6** showed a high Φ_f value.

In addition, we investigated the fluorescence stability of the three compounds in dimethyl sulfoxide for 300 seconds (Fig. 2b). Due to the limitation of the instrument, if the excitation wavelength of 500 nm and the emission wavelength of 560 nm are used, the fluorescence intensity of the compound is beyond the measurement range of the fluorescence spectrophotometer. Therefore, we set a relatively appropriate excitation wavelength of 430

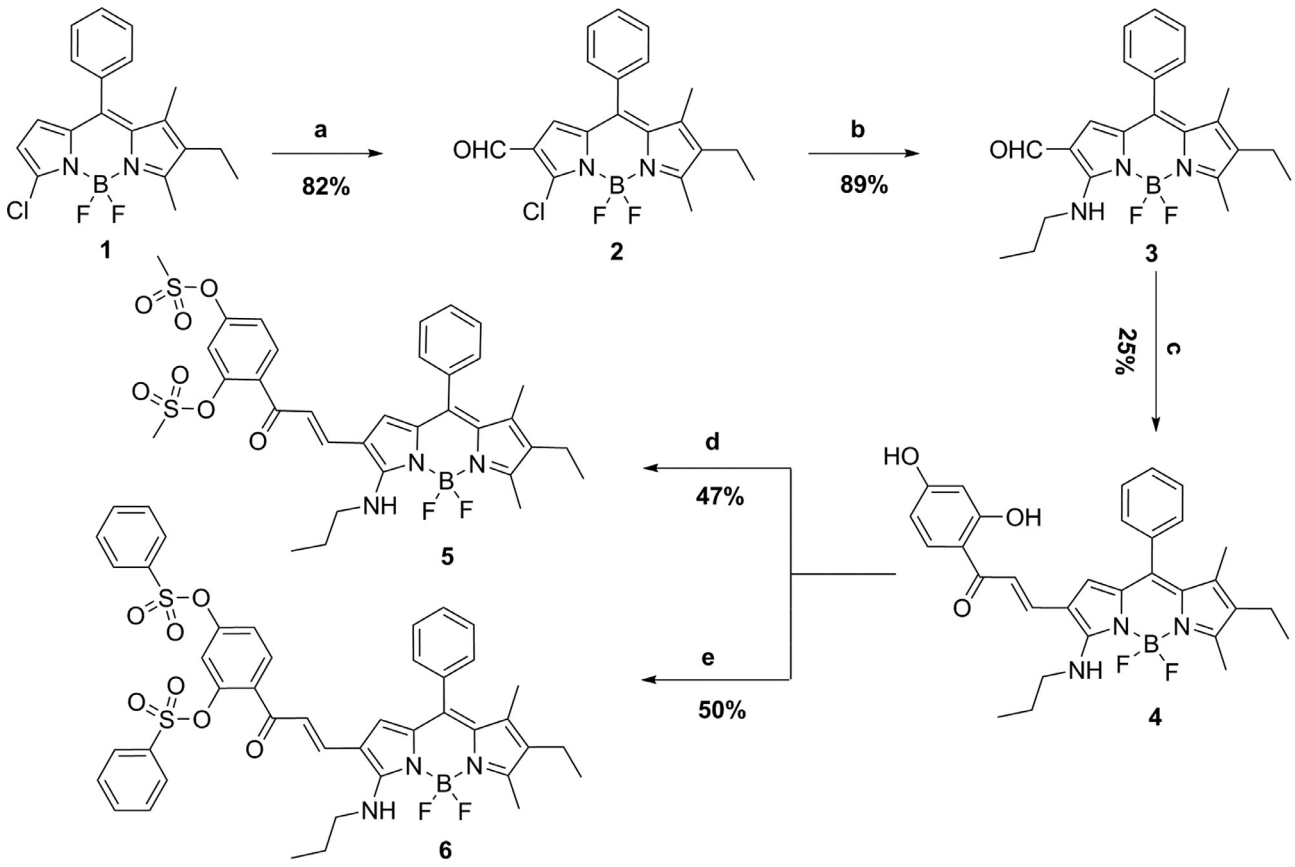

Scheme 1. Synthetic route of bis-sulfonyl chalcone-BODIPY.

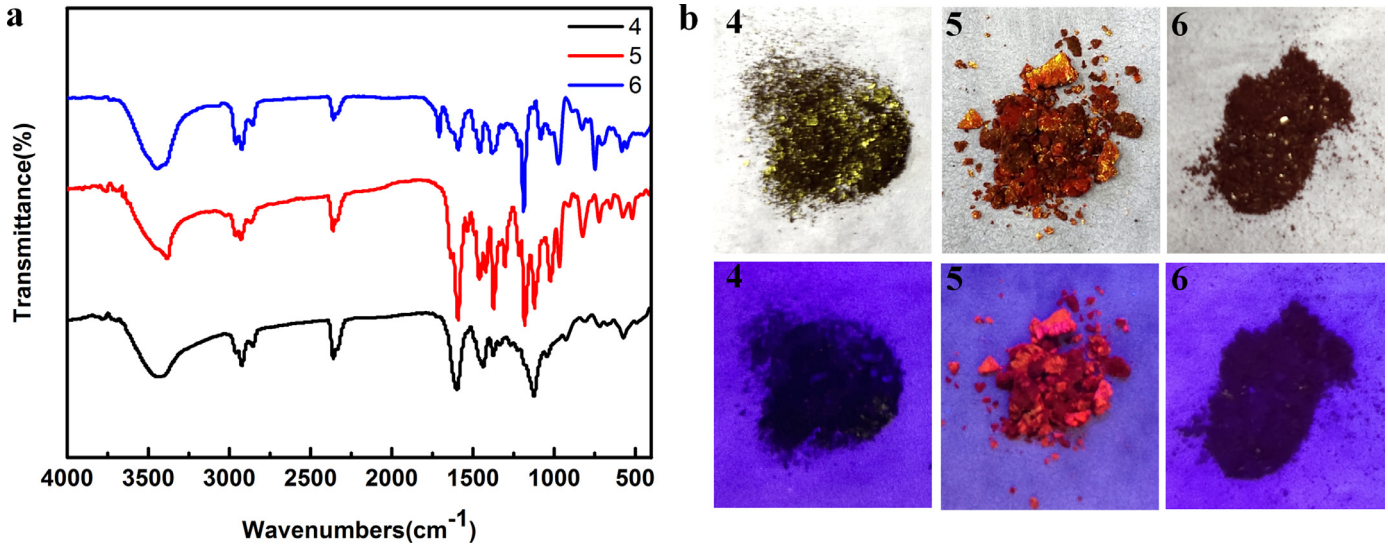

Fig. 1. (a)The infrared spectrogram of compounds **4, 5, 6** measured by KBr tablet. (b) Pictures of **4-6** solids in sunlight (upper) and 365 nm ultraviolet lamp (lower).

Table 1
Photophysical properties of compounds **4-6**.

Compounds	$\lambda_{max(abs)}$ [nm]	Emission [nm]	Stokes shift [nm]	Stokes shift [cm^{-1}]	Φ_f[a]
4	545	569	24	774	0.22
5	548	569	21	673	0.25
6	540	566	26	850	0.31

[a] Fluorescence quantum yield estimated relative to rhodamine B as the standard (Φ_f = 0.65 in ethanol).

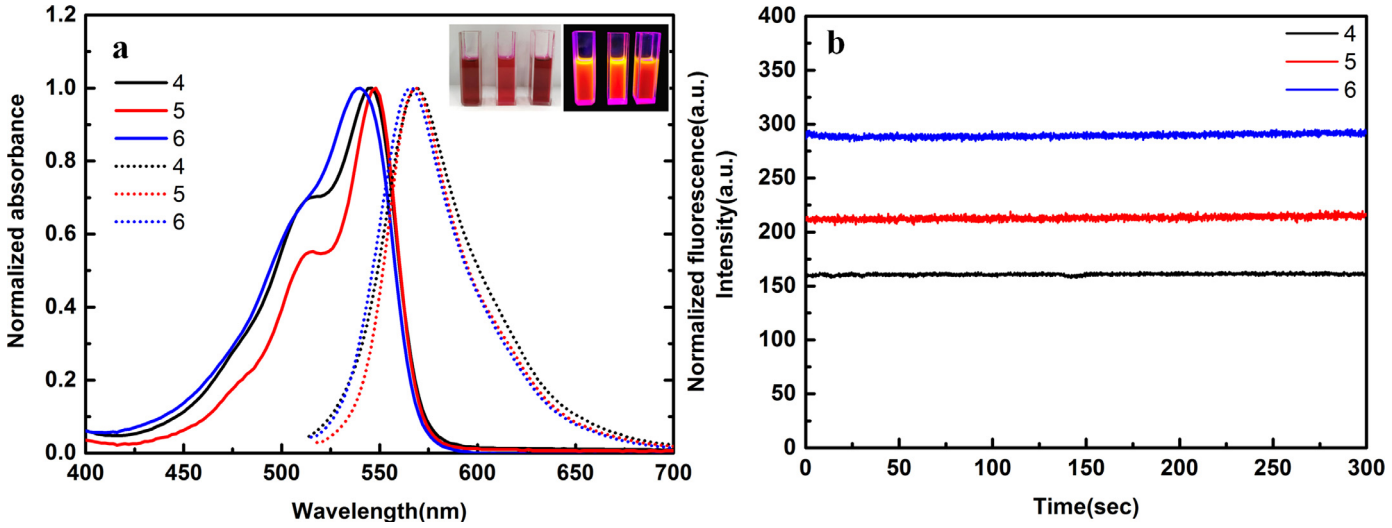

Fig. 2. (a) The solid line is the normalized UV-Vis spectrum of compounds **4**-**6** in dichloromethane solution (10 μM), and the dashed line is the normalized fluorescence spectrum of compounds (2 μM) (excitation wavelength = 500 nm). Compounds **4**-**6** in sunlight (left) and uv light (right) are shown in the upper right. (b) The fluorescence stability of BODIPY derivatives **4**-**6** in dimethyl sulfoxide at concentrations of 2.0 μmol L^{-1} (excitation wavelength = 430 nm, emission wavelength = 560 nm).

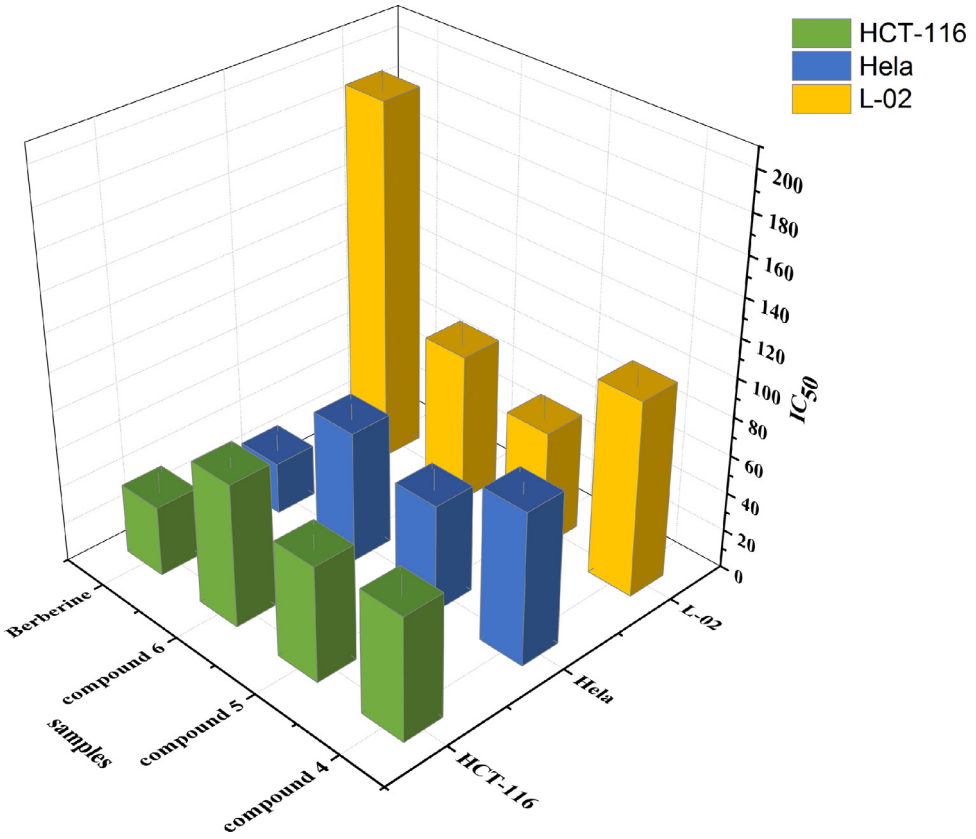

Fig. 3. Stereoscopic histogram of IC_{50} of different compounds.

nm. Obviously, the three compounds remained dynamically stable over time in the dimethyl sulfoxide solvent.

3.3. Cytotoxicity studies

Compounds **4, 5** and **6** were used to conduct the cell activity of HCT-116, HeLa and L-02 cells, respectively (Table 2 and Fig. 3). It can be found that the toxicity of compound **4** was relatively low after the introduction of chalcone to BODIPY, and the IC_{50} value of normal cells L-02 was 102.21. The IC_{50} value of compound **5** decreased from 79.71±3.84 μmol L^{-1} to 56.10±8.51 μmol L^{-1} and compound **6** to 68.47±5.34 μmol L^{-1} after introducing bis-sulfonyl group, indicating that the introduction of sulfonyl group could improve the efficacy of the compound. Among them, the effect of **5** was more obvious.

3.4. Cellular imaging and in vivo imaging

Further study on the cell imaging of BODIPY derivatives (Fig. 4A and B) shows that compounds **5** and **6** are highly overlapped with

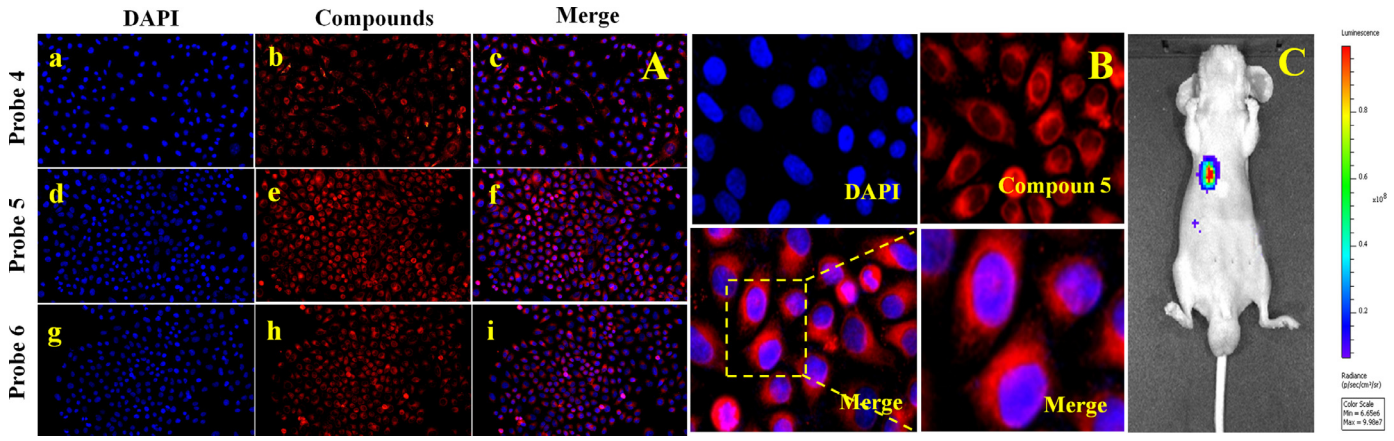

Fig. 4. (A) HeLa cells were fixed in paraformaldehyde solution, incubated with DAPI in dark, and nuclear imaging under fluorescence microscope (blue), different compounds at a concentration of 2.5 μmol L^{-1} (red) and merged image. Compound **4**: a-c; Compound **5**: d-f; Compound **6**: g-i. (B) Magnified view of d-f cell imaging. (C) *In vivo* imaging of compound **5** in mice.

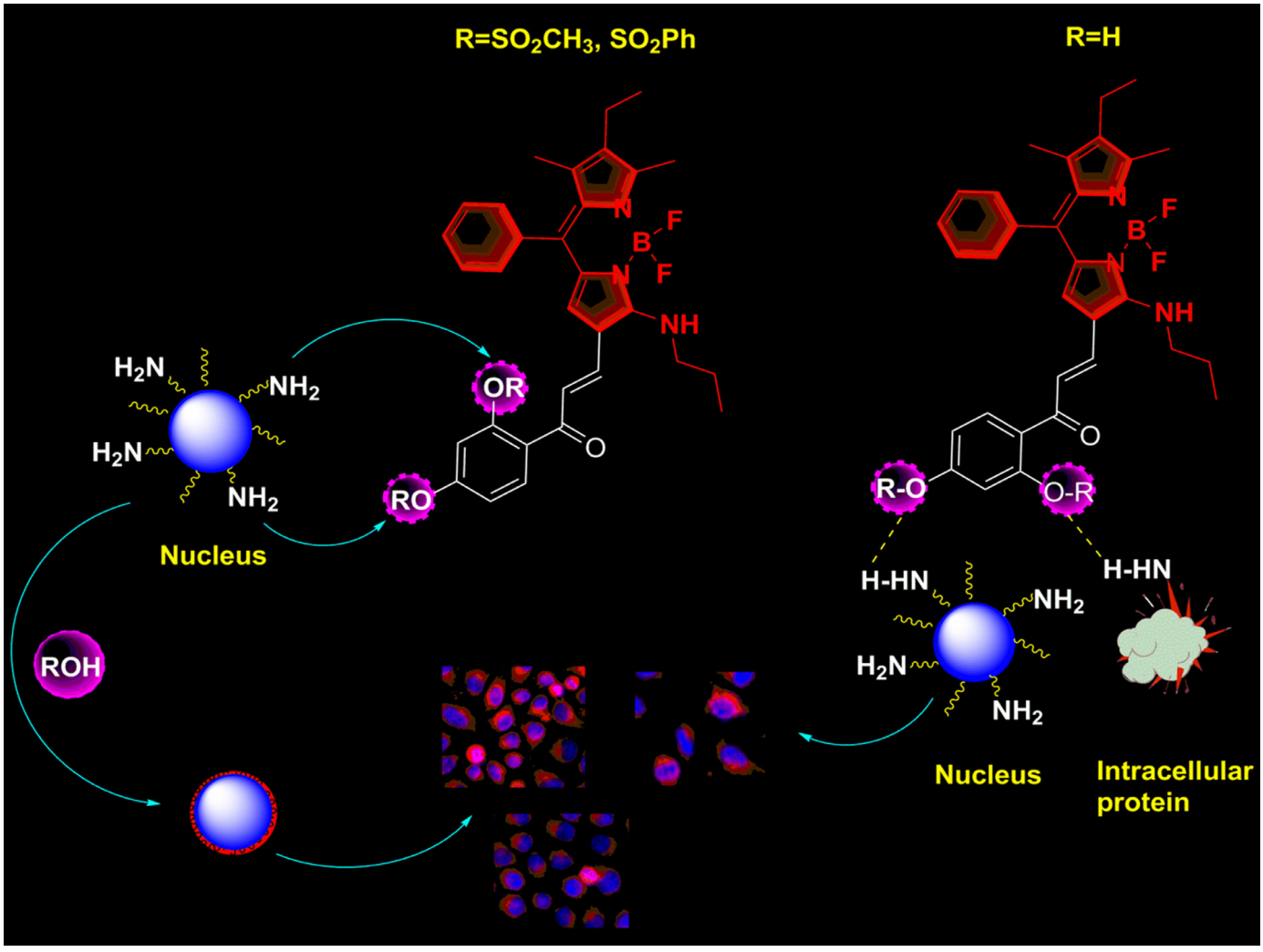

Fig. 5. Cellular imaging mechanism.

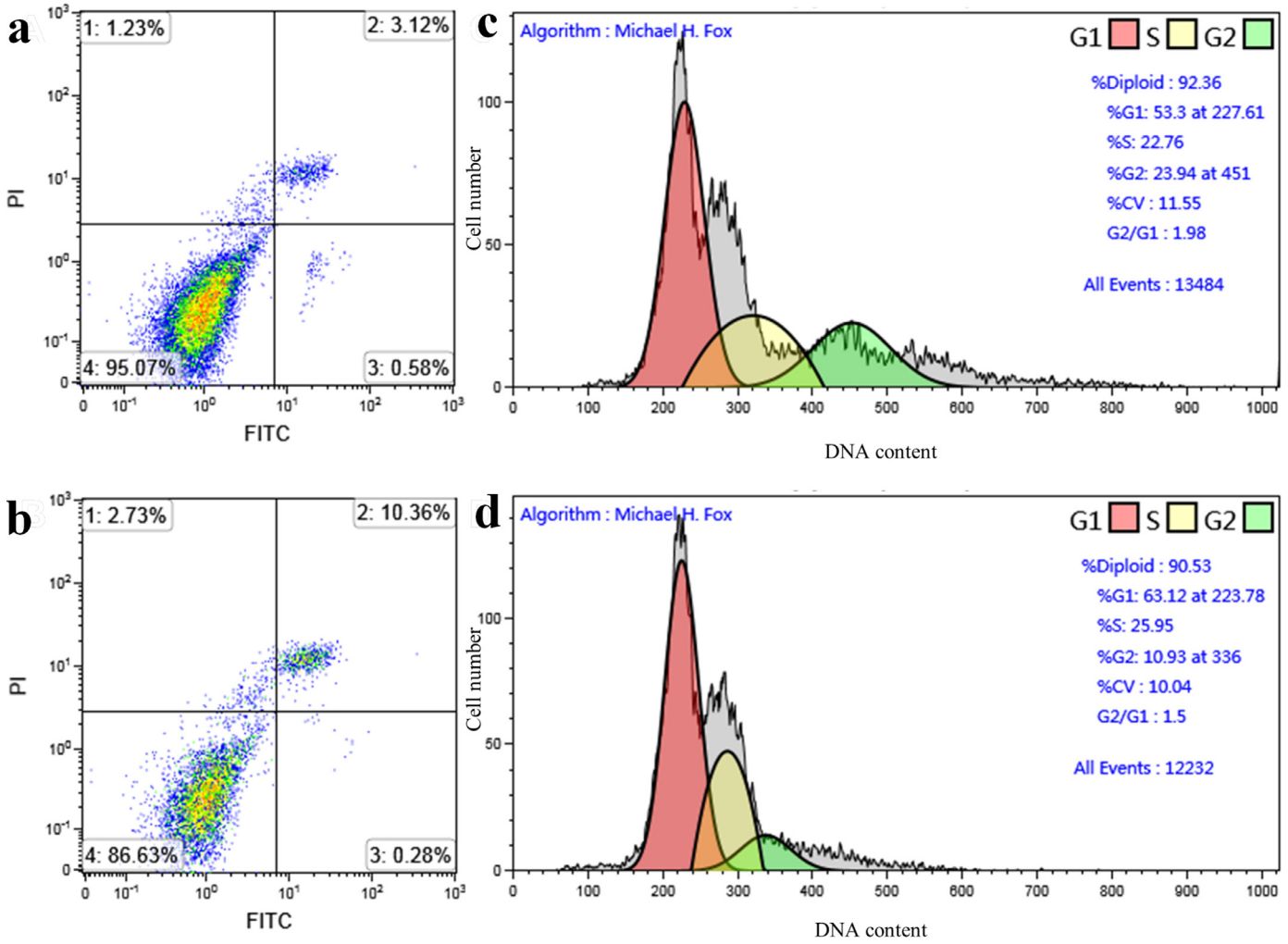

Fig. 6. (a) HeLa cells were incubated with compound **5** and Berberine for 12 h, stained with PI and annexin-V / FITC, and then analyzed by flow cytometry analysis. Early apoptotic cells are shown in the lower right quadrant. (b) Apoptosis rate of HeLa cells under Berberine. (c) The flow cytometry of HeLa cells treated with compound **5** was analyzed using ModFit LT2.0 software. (d)The flow cytometry of berberine was used as control.

Table 2
Experimental data of cytotoxicity.

Compounds	IC_{50} (μmol L^{-1}) ± SD		
	HCT-116	HeLa	L-02
4	64.33±8.36	79.71±3.84	102.21±5.97
5	60.33±4.31	56.10±8.51	61.29±10.12
6	74.86±2.77	68.47±5.34	78.22±9.88
Berberine	36.56±7.86	27.07±5.56	188.82±8.09

the nuclei of HeLa cells, indicating that compounds **5** and **6** completely entered the cell nucleus. However, a small part of compound **4** is free from the nucleus. It may be that compound **4** contains two hydroxyl groups, which can easily form hydrogen bonds with proteins in cells, resulting in some compounds dissociating outside the nucleus (Fig. 5). For compounds **5** and **6**, when methylsulfonyl group and phenylsulfonyl group replace the hydrogen atoms on the hydroxyl group, they enter the cell and react with the amino acids in the nucleus, thus leaving the sulfonyl group [31, 32]. Under the fluorescence microscope, they fully combine with HeLa nucleus. After the introduction of double sulfonyl group, the compound only binds to the tumor nucleus for imaging, which shows the excellent biocompatibility and targeting property of the dye.

Since the introduction of dimethylsulfonyl group has a greater effect on IC_{50} value than benzene sulfonyl group and has more obvious inhibitory effect on cancer cells, **5** was used for basic imaging *in vivo* in mice in order to further enhance the follow-up biological research. The fluorescence intensity of the subcutaneous tumor tissue was detected after injection of compound **5** in mice (Fig. 4C) 30 minutes. The *in vivo* imaging showed a strong fluorescence in the tumor tissue, which directly demonstrated the potential targeting of the compound to tumor cells.

3.5. Flow cytometry analysis of HeLa cells apoptosis

Annexin V / PI double staining was used to identify early and late apoptotic cells, dead cells and living cells [33–36], and the apoptosis rate was quantified. The experiment was repeated three times independently. The lower left quadrant (annexin V negative - PI negative) represents normal cells (Fig. 6a and b). After compound **5** treatment, the percentage of living cells was 95.07%. The early apoptosis rate and late apoptosis rate were 0.58% and 0.58% respectively, although the apoptotic cell rate of 3.7% was lower than that of berberine (10.64%), it would be a breakthrough in BODIPY probe cell experiment.

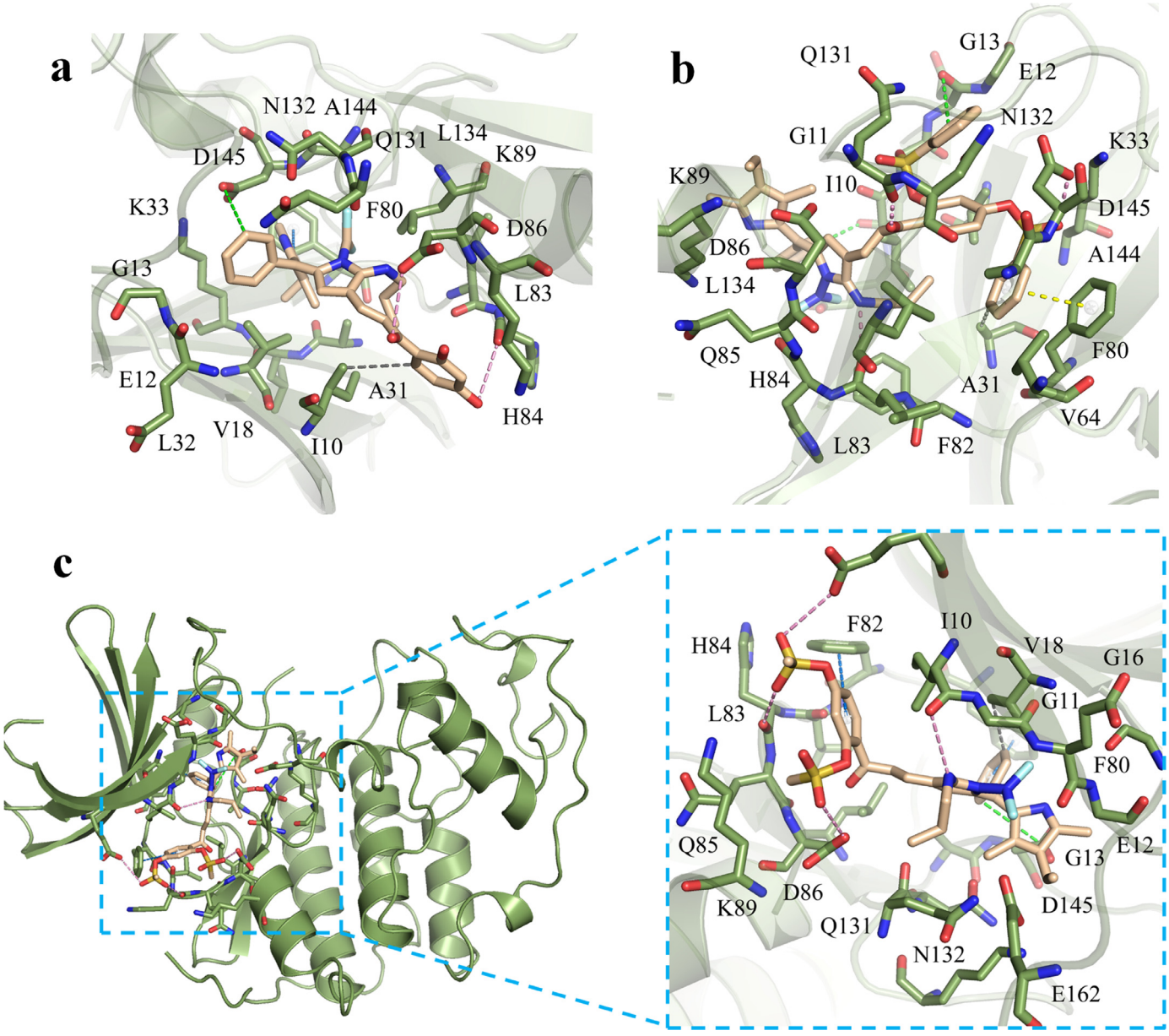

Fig. 7. molecular docking diagram of different compounds with CDK2. (a) Compound **4**. (b) Compound **6**. (c) Compound **5**.

3.6. Compound 5 induced mitotic block in HeLa cells

The effect of compound **5** on HeLa cells proliferation was investigated by flow cytometry (Fig. 6c and d). The experiment was independently repeated three times. The average DNA content in G1 phase was 223.78, and the number of cells in G1 phase accounts for 63.12% of the total. At this time, the number of cells was the most, but the DNA content was the least. In the S phase, DNA began to replicate to complete replication, and the DNA content multiplied. Therefore, the S phase shows a particularly long span in the result chart. Compared with the cells treated with control [37], HeLa cells treated with compound **5** caused 22.76% s phase stagnation, which was higher than the blank control. This data well demonstrated the inhibitory effect of compound **5** on S phase in cell division. The data of S was lower than 25.95% of berberine, which corresponded with apoptosis experiment.

3.7. Molecular docking

In order to elucidate the mechanism of action of these three compounds on tumor cells, molecular docking simulations of tumor target CDK2 kinases were performed (Fig. 7) [38–41]. Affinity Score is one of the standard to measure the docking results (Table 3). The binding energy of compound **5** and **6** is -8.4 and -8.6 kcal•mol^{-1}, respectively, which is higher than compound **4**. This indicates that the introduction of disulfonyl group increases the affinity of CDK2, making it easier to bind to cells. However, compounds **5** and **6** have similar binding energies, so we have analyzed their main forces. The benzene ring on the BODIPY parent nucleus in compound **5** formed a T-π accumulation with Phe 80, and the benzene ring directly attached to the dimethyl sulfonyl group also formed a T-π interactions with the residue Phe 82, while compound **6** only contained one. The benzene ring directly connected with bis-phenylsulfonyl group of compound **6** forms π

Table 3
Interaction between residues and compounds (PDBID: 2FVD).

Entry	Affinity score	Interaction with receptor				
(PDBID 2FVD)	(kcal•mol^{-1})	[H]	π-π	T-π	Ion-Pi	Hydrophobic bond
4	-7.0	His 84 Asp 145		Phe 80	Asp 86 Asp 145 Lys 89 His 84 GLU12	Ala 31 Ala 144 Ile 10 Phe 80
5	-8.4	Glu 8 Gln 85 Gln131 Ile 10		Phe 80 Phe 82	Asp 145 Glu 8 Glu 12 Glu 162 His 84 Lys 89	Ala 144 Leu 83 Phe 80 Phe 82 Val 18
6	-8.6	Asp 145 Gln 131 Leu 83	Phe 80	Phe 82	Asp 86 Glu 12 His 84 Lys 9	Ala 31 Leu 83 Leu 134 Phe 80 Phe 82

- π stacking with Phe 80. In addition, compound **5** has more hydrogen bonds and ion-Pi interactions with CDK2 than compound **6**, so compound **5** may have a slightly stronger binding capacity with cells by comparing the interactions.

4. Conclusion

In conclusion, we have successfully synthesized bis-sulfonyl chalcone-BODIPY target cell fluorescent probes. The probe has excellent cellular permeability and promising targeting properties. The easy leaving bis-sulfonyl group is a highlight of this design, because its presence leads to excellent binding ability to target cells in cellular imaging of the compound, *in vivo* imaging and molecular docking in mice. In addition, as a probe, it also has the potential antitumor properties of chalcone derivatives. Cell activity experiment showed that the introduction of disulfonyl group could enhance the inhibitory effect of the probe on tumor cells. Flow cytometry also showed that they could promote the apoptosis of HeLa cells and inhibit the proliferation of cancer cells. Finally, this design can provide a basis for the future research of bis-functional drug-fluorescent probes with better biocompatibility and low cytotoxicity.

Declaration of Competing Interest

The authors declare that they have no known competing financial interests or personal relationships that could have appeared to influence the work reported in this paper.

CRediT authorship contribution statement

Zhixiang Lv: Investigation, Data curtion, Formal analysis, Writing – original draft. **Yuling Wang:** Investigation, Visualization, Validation. **Jinliang Zhang:** Investigation. **Zhou Wang:** Methodology. **Guofan Jin:** Conceptualization, Methodology, Writing – review & editing, Project administration.

Acknowledgements

We would like to thank the scientific research foundation of Jiangsu University (Grant No. 5501290005) for the financial supports. Thanks again for the biological experimental data provided by the affiliated Danyang Hospital of Nantong University and Zhucheng Maternal and Child Health Hospital.

Supplementary materials

Supplementary material associated with this article can be found, in the online version, at doi:10.1016/j.molstruc.2021.130201.

References

[1] D. Choi, J.C. Park, H.N. Lee, J.H. Moon, H.W. Ahn, K. Park, J. Hong, In vitro osteogenic differentiation and antibacterial potentials of chalcone derivatives, Mol. Pharmaceutics 15 (2018) 3197–3204, doi:10.1021/acs.molpharmaceut.8b00288.
[2] X. Zhang, K.P. Rakesh, S.N.A. Bukhari, M. Balakrishna, H.M. Manukumar, H.L. Qin, Multi-targetable chalcone analogs to treat deadly Alzheimer's disease: Current view and upcoming advice, Bioorg. Chem. 80 (2018) 86–93, doi:10.1016/j.bioorg.2018.06.009.
[3] L. Wang, Y. Wang, Y. Tian, J. Shang, X. Sun, H. Chen, H. Wang, W. Tan, Design, synthesis, biological evaluation, and molecular modeling studies of chalcone-rivastigmine hybrids as cholinesterase inhibitors, Bioorgan. Med. Chem. 25 (2017) 360–371, doi:10.1016/j.bmc.2016.11.002.
[4] P. Cheng, L. Yang, X. Huang, X. Wang, M. Gong, Chalcone hybrids and their antimalarial activity, Arch. Pharm. 353 (2020) 1900350, doi:10.1002/ardp.201900350.
[5] S.L. Gaonkar, U.N. Vignesh, Synthesis and pharmacological properties of chalcones: a review, Res. Chem. Intermed. 43 (2017) 6043–6077, doi:10.1007/s11164-017-2977-5.
[6] C.M. So, Z. Zhou, C.P. Lau, F.Y. Kwong, Palladium-catalyzed amination of aryl mesylates, Angew Chem., Int. Ed. Engl. 47 (2008) 6402–6406, doi:10.1002/anie.200802157.
[7] P. Kumar Reddy Nagireddy, V. Krishna Kommalapati, V. Siva Krishna, D. Sriram, A. Devi Tangutur, S. Kantevari, Anticancer potential of N-sulfonyl noscapinoids: Synthesis and evaluation, ChemistrySelect 5 (2020) 2972–2980, doi:10.1002/slct.202000142.
[8] J.M. Franke, B.K. Raliski, S.C. Boggess, D.V. Natesan, E.T. Koretsky, P. Zhang, R.U. Kulkarni, P.E. Deal, E.W. Miller, BODIPY fluorophores for membrane potential imaging, J. Am. Chem. Soc. 141 (2019) 12824–12831, doi:10.1021/jacs.9b05912.
[9] J.M. Dorn, M. Alpern, C. McNulty, G.W. Volcheck, Curr. Sulfonamide drug allergy, Curr. Allergy Asthm. 18 (2018) 38, doi:10.1007/s11882-018-0791-9.
[10] L. Sun, C. Wang, X. Hu, Y. Wu, Z. Jiang, Z. Li, X. Chen, L. Hu, Design, synthesis, and evaluations of the antiproliferative activity and aqueous solubility of novel carbazole sulfonamide derivatives as antitumor agents, Bioorg. Chem. 99 (2020) 103766, doi:10.1016/j.bioorg.2020.103766.
[11] W. Janssens, M. Bafadhel, The CICERO (collaboration in COPD exacerbations) clinical research collaboration, Eur. Respir. J. 55 (2020) 2000079, doi:10.1183/13993003.00079-2020.
[12] C. Wijesooriya, J. Peterson, P. Shrestha, E. Gehrmann, A. Winter, E. Smith, Photoactivatable BODIPY probe for localization-based super-resolution cellular imaging, Angew. Chem. (2018) 130, doi:10.1002/ange.201805827.
[13] S. Qi, N. Kwon, Y. Yim, V.N. Nguyen, J. Yoon, Fine-tuning the electronic structure of heavy-atom-free BODIPY photosensitizers for fluorescence imaging and mitochondria-targeted photodynamic therapy, Chem. Sci. 11 (2020) 6479–6484, doi:10.1039/D0SC01171A.
[14] Z. Shahroosvand, N.R. Yeganeh, S. Haddadian, J. Farzaneh, M.S. Ardestani, PLGA-methionine labeled BODIPY nano-conjugate for in-vivo optical tumor imaging, Appl. Nanosci. 10 (2020) 1441–1452, doi:10.1007/s13204-019-01232-w.
[15] J.X. Chen, W.W. Tao, W.C. Chen, Y.F. Xiao, K. Wang, C. Cao, J. Yu, S. Li, F.X. Geng, C. Adachi, C.S. Lee, X.H. Zhang, Red/near-infrared thermally activated delayed

fluorescence oleds with near 100 % internal quantum efficiency, Angew. Chem., Int. Ed. 58 (2019) 14660–14665, doi:10.1002/anie.201906575.
[16] X. Kong, L. Di, Y. Fan, Z. Zhou, X. Feng, L. Gai, J. Tian, H. Lu, Lysosome-targeting turn-on red/NIR BODIPY probes for imaging hypoxic cells, Chem. Commun. 55 (2019) 11567–11570, doi:10.1039/C9CC04416G.
[17] Z. Ye, C. Xiong, J. Pan, D. Su, L. Zeng, Highly photostable, lysosome-targeted BODIPYs with green to near-infrared emission for lysosome imaging in living cells, Dyes Pigm 155 (2018) 30–35, doi:10.1016/j.dyepig.2018.03.015.
[18] R. Prieto-Montero, A. Prieto-Castañeda, R. Sola-Llano, A.R. Agarrabeitia, D. García-Fresnadillo, I. López-Arbeloa, A. Villanueva, M.J. Ortiz, S. de la Moya, V. Martínez-Martínez, Exploring BODIPY derivatives as singlet oxygen photosensitizers for PDT, Photochem. Photobiol. 96 (2020) 458–477, doi:10.1111/php.13232.
[19] W. Gao, M. Li, G. Xu, R. Wang, B. Shi, J. Gao, X. Gu, P. Shi, C. Zhao, Tumor microenvironment-activated nanosystems with selenophenol substituted BODIPYs as photosensitizers for photodynamic therapy, Bioorg. Med. Chem. Lett. 30 (2019) 126854, doi:10.1016/j.bmcl.2019.126854.
[20] K.S. Choung, K. Marroquin, T.S. Teets, Cyclometalated iridium-BODIPY ratiometric O_2 sensors, Chem. Sci. 10 (2019) 5124–5132, doi:10.1039/C9SC00696F.
[21] A.C. Sedgwick, R.S.L. Chapman, J.E. Gardiner, L.R. Peacock, G. Kim, J. Yoon, S.D. Bull, T.D. James, A bodipy based hydroxylamine sensor, Chem. Commun. 53 (2017) 10441–10443, doi:10.1039/C7CC05872A.
[22] J.S. Hansen, T. Hoeg-Jensen, J.B. Christensen, Redemitting BODIPY boronic acid fluorescent sensors for detection of lactate, Tetrahedron 73 (2017) 3010–3013, doi:10.1016/j.tet.2017.04.019.
[23] P.E. Kesavan, V. Pandey, M.K. Raza, S. Mori, I. Gupta, Water soluble thioglycosylated BODIPYs for mitochondria targeted cytotoxicity, Bioorg. Chem. 91 (2019) 103139, doi:10.1016/j.bioorg.2019.103139.
[24] F. Sun, G. Yang, Q. Zhang, Z. Xue, C. Gu, Z. Chen, B. Yan, Y. Feng, Z. Wang, S. Meng, The self-assembly of monosubstituted BODIPY and HFBI-RGD, RSC Adv 8 (2018) 21472–21479, doi:10.1039/C8RA03687J.
[25] M. Li, R. Tian, J. Fan, J. Du, S. Long, X. Peng, A lysosome-targeted BODIPY as potential NIR photosensitizer for photodynamic therapy, Dyes Pigm 147 (2017) 99–105, doi:10.1016/j.dyepig.2017.07.048.
[26] W. Hu, H. Ma, B. Hou, H. Zhao, Y. Ji, R. Jiang, X. Hu, X. Lu, L. Zhang, Y. Tang, Q. Fan, W. Huang, Engineering lysosome-targeting BODIPY nanoparticles for photoacoustic imaging and photodynamic therapy under near-infrared light, ACS Appl. Mater. Interfaces 8 (2016) 12039–12047, doi:10.1021/acsami.6b02721.
[27] C. Zhao, J. Zhang, X. Wang, Y. Zhang, Pyridone fused boron-dipyrromethenes: synthesis and properties, Org. Biomol. Chem. 11 (2013) 372–377, doi:10.1039/c2ob26791h.
[28] N. Zhao, M.G.H. Vicente, F.R. Fronczek, K.M. Smith, Pyridone fused boron-dipyrromethenes: synthesis and properties. Synthesis of 3,8-Dichloro-6-ethyl-1,2,5,7-tetramethyl–BODIPY from an asymmetric dipyrroketone and reactivity studies at the 3,5,8-positions, Chem. - Eur. J. 21 (2015) 6181–6192, doi:10.1002/chem.201406550.
[29] A. Poirel, A. De Nicola, P. Retailleau, R. Ziessel, Oxidative coupling of 1,7,8-unsubstituted BODIPYs: Synthesis and electrochemical and spectroscopic properties, J. Org. Chem. 77 (2012) 7512–7525, doi:10.1021/jo301300b.
[30] X. Dong, G. Deng, J. Xu, H. Li, X. Zeng, Decomposition of sulfonyl azide isocyanate and sulfonyl diazide: The oxygen-shifted curtius rearrangement via sulfonyl nitrenes, J. Phys. Chem. A 122 (2018) 8511–8519, doi:10.1021/acs.jpca.8b06655.
[31] L. Wang, Y. Qian, A novel quinoline-BODIPY fluorescent probe for fast sensing biothiols via hydrogen bonds assisted-deprotonation mechanism and its application in cells and zebrafish imaging, J. Photochem. Photobiol., A 372 (2019) 122–130, doi:10.1016/j.jphotochem.2018.12.013.
[32] H. Guo, Y. Jing, X. Yuan, S. Ji, J. Zhao, X. Li, Y. Kan, Highly selective fluorescent OFF-ON thiol probes based on dyads of BODIPY and potent intramolecular electron sink 2,4-dinitrobenzenesulfonyl subunits, Org. Biomol. Chem. 9 (2011) 3844–3853, doi:10.1039/c0ob00910e.
[33] P. Ashokkumar, A.H. Ashoka, M. Collot, A. Das, A.S. Klymchenko, A fluorogenic BODIPY molecular rotor as an apoptosis marker, Chem. Commun (Camb). 55 (2019) 6902–6905, doi:10.1039/c9cc03242h.
[34] E. Indrigo, J. Clavadetscher, S.V. Chankeshwara, A. Lilienkampf, M. Bradley, Palladium-mediated in situ synthesis of an anticancer agent, Chem. Commun (Camb). 52 (2016) 14212–14214, doi:10.1039/c6cc08666g.
[35] C.F. Hagert, A.B. Bohn, T.R. Wittenborn, S.E. Degn, Seeing the confetti colors in a new light utilizing flow cytometry and imaging flow cytometry, Cytometry A 97 (2020) 811–823, doi:10.1002/cyto.a.24032.
[36] E. Kim, H. Koo, Biomedical applications of copper-free click chemistry: in vitro, in vivo, and ex vivo, Chem. Sci. 10 (2019) 7835–7851, doi:10.1039/c9sc03368h.
[37] D. Raghav, S.M. Ashraf, L. Mohan, K. Rathinasamy, Berberine induces toxicity in HeLa cells through perturbation of microtubule polymerization by binding to tubulin at a unique site, Biochemistry 56 (2017) 2594–2611, doi:10.1021/acs.biochem.7b00101.
[38] P. Ayaz, D. Andres, D.A. Kwiatkowski, C.C. Kolbe, P. Lienau, G. Siemeister, U. Lucking, C.M. Stegmann, Conformational adaption may explain the slow dissociation kinetics of roniciclib (BAY 1000394), a Type I CDK inhibitor with kinetic selectivity for CDK2 and CDK9, ACS Chem. Biol. 11 (2016) 1710–1719, doi:10.1021/acschembio.6b00074.
[39] G. Chakraborty, A.K. Ray, P.K. Singh, H. Pal, Non-covalent interaction of BODIPY-benzimidazole conjugate with bovine serum albumin-A photophysical and molecular docking study, J. Photochem. Photobiol., A 377 (2019) 220–227, doi:10.1016/j.jphotochem.2019.04.001.
[40] A.A. Ksenofontov, P.S. Bocharov, E.V. Antina, Interaction of tetramethyl-substituted BODIPY dye with bovine serum albumin: Spectroscopic study and molecular docking, J. Photochem. Photobiol., A 368 (2019) 254–257, doi:10.1016/j.jphotochem.2018.10.002.
[41] D.M. Aziz, H.J. Azeez, Synthesis of new ß-lactam- N-(thiazol-2-yl)benzene sulfonamide hybrids: Their in vitro antimicrobial and in silico molecular docking studies, J. Mol. Struct. 1222 (2020) 128904, doi:10.1016/j.molstruc.2020.128904.